Velocity Measurements of Doorway Flow Induced by an Air Curtain

Adam J. Pierce, [*] Takayuki Yajin,[*] Vijay A. Chauhan,[†] Frank K. Lu,[‡] and J. Craig Dutton[§]

University of Texas at Arlington, Arlington, TX, 76019

The airflow induced by an air curtain mounted over a doorway is examined for its potential use in explosive detection portals. A challenge to gaining understanding of such flows is mapping it using particle image velocimetry (PIV), a technique which is usually used in smaller-scale applications and with higher velocity flows. This paper discusses some of the challenges, requirements, techniques, and results of mapping large-scale flows with PIV, in particular, the mapping of a doorway flow induced by an air curtain.

Nomenclature

EDP	= explosive detection portal	T_x	= translation in *x* direction
PIV	= particle image velocimetry	T_y	= translation in *y* direction
AOI	= area of interest	T_z	= translation in *z* direction
CCD	= charge-coupled device	R_x	= rotation in *x* direction
RMS	= root-mean-square	R_y	= rotation in *y* direction
		R_z	= rotation in *z* direction

I. Introduction

EXPLOSIVE detection portals (EDPs) are increasingly being deployed in airports and are expected to see further widespread use in entrances to indoor public places such as shopping centers, office complexes and public transport nodes, such as bus, train and subway stations.[1] Most of the existing EDP designs, however, tend to be highly intrusive and at times even startling to the unwary subject. For example, some of these designs use a series of brief puffer jets to loosen material from the subject. Thus, the development of less intrusive EDPs can produce wider acceptance by the general public as government authorities tackle the threat of terrorist attacks on so-called soft targets.

One approach for reducing the intrusiveness of EDPs is to reduce the strength of the air puffs or even to eliminate them altogether. Gowadia and Settles[2] have suggested that it is possible to detect airborne trace substances through sampling the flow from the natural convection past a human subject, even through various types of clothing, with some assistance from puffer jets; see also Settles.[3] This suggestion is important in developing less intrusive EDPs. Natural convection, although weaker than the puffs of air jets commonly used to dislodge trace substances, may still be able to loosen sufficient trace materials to be detected by advanced sensors capable of detection at the parts per trillion level.

A possible approach to reduced intrusion of EDPs is to provide a weak, steady airflow past the subject instead of merely relying on natural convection. An example was proposed by Parmeter et al.[4] Another possible solution may be provided by using air curtains to generate flow past the human subject. A collection and concentrator system can

[*]Undergraduate Research Assistant, Mechanical and Aerospace Engineering Department, Box 19018. AIAA Student Member.

[†]Graduate Student, Mechanical and Aerospace Engineering Department, Box 19018; currently, Product and Development Engineer, Flow Design, Inc., Dallas, Texas..

[‡]Professor and Director, Aerodynamics Research Center, Mechanical and Aerospace Engineering Department, Box 19018. AIAA Associate Fellow.

[§]Professor and Chair, Mechanical and Aerospace Engineering Department, Box 19018. AIAA Associate Fellow.

then be used to collect an air sample for analysis. Air curtains of different sizes, volumetric flow rates and air speeds, which are found in various applications for energy savings, air quality and temperature control in public areas, and contaminant transport, have found general acceptance by the public.[5-11] More specialized uses of air curtains include refrigeration,[12.13] mining,[14] and the food and semiconductor industries.[15,16]

In the proposed concept, the EDP is an integral part of a doorway, on top of which is mounted an air curtain. The airflow is received by a floor-mounted receiver. It may prove to be advantageous to combine the flow from an air curtain with the human aerodynamic wake[7] for trace material detection. This paper explores techniques for mapping the airflow within the doorway using particle image velocimety (PIV). Some of the topics to be discussed are the development of the flow facility, the PIV system, calibration techniques, and other factors that require close attention. Preliminary results of the PIV measurements are also presented.

II. Experimental Setup

A. Flow Facility

There were several requirements that needed to be fulfilled in order for the experiment to be successful. The first was to design and fabricate an appropriate flow facility with the necessary optical access so that the flow field could be examined in detail. A second requirement was to determine and implement a measurement method that would achieve the goal of mapping the flow field, so that it can be better understood and appropriate EDP design guidelines could be suggested.

For simplicity of fabrication and minimal cost, it was decided early on to use materials and construction methods for the flow facility that are typical of those used in home construction. The results of the design considerations were to construct a typical doorway that is approximately 3 ft. wide by 7 ft. tall by 6 in. thick and to place this doorway in a structure such that a PIV system would be capable of analyzing the air flow.

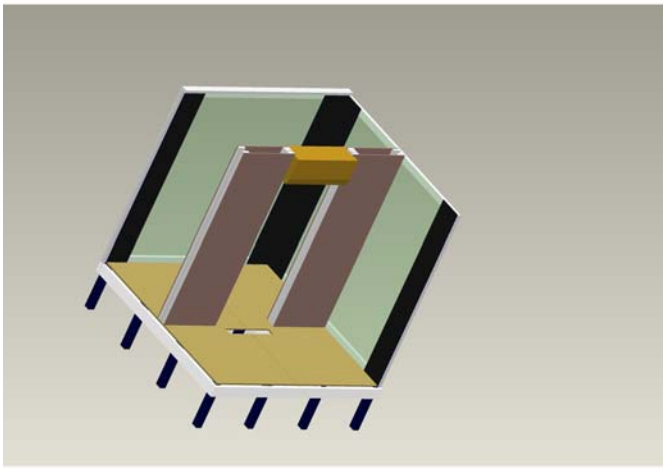

Fig. 1. Cutaway view of test cabin. The color variation is for orientation only.

The cabin was first designed and drawn using the CAD program ProEngineer Wildfire in order to ensure proper fit of the components and to identify any potential complications that might occur during construction. The layout of the air cabin is an 8 ft. cube consisting of a floor, walls, ceiling and the doorway. Figure 1 is a cutaway view of the cabin at the final design stage. The missing walls that are not shown are similar to their adjacent counterparts shown in Fig. 1. The materials used to construct the frame of the cabin are common construction pine that can be found at most hardware stores. The transparent portions of the walls, shown as a light green tint in Fig. 1, are transparent GE Lexan sheets, which are 36 in. by 96 in. by 0.5 in. thick. Lexan was chosen due to its higher transparency and durability compared to typical Plexiglas. Glass was also considered, but due to its size, thickness, and excessive load on the structure, it was not chosen.

An air curtain blower unit is mounted approximately 6 ft. above the floor near the doorway in the center of the cabin. The air curtain is a Fantech model AC3600 that is capable of producing 795 cfm of flow. For the present setup, the exhaust port of the air curtain is set just forward of the doorway and blows vertically downward. This allows the PIV system to collect data in the center plane of the air curtain flow. Subsequent experiments may consider other positions of the air curtain relative to the doorway.

The cabin is raised 2 ft. above the ground so that any modifications to the cabin's floor or support system could be made as needed. A small rectangular slot was cut in the floor of the cabin for an exhaust vent so that ventilation ducts could be installed from outside the cabin for recirculation of the air curtain flow, thereby allowing a closed environment for the PIV seeding. This recirculation system also simulates the method by which air would be collected and then processed for explosives detection. The cabin, in its final constructed form, is shown in Fig. 2. The figure shows the front of the test cabin. In front of the cabin are placed the two cameras of the stereo PIV system. The laser for the PIV system is just to the right of the cabin.

B. PIV System

The next task was to arrange the PIV system for data collection. The PIV system used in this study was from LaVision. The system includes two Flow Master 3S Image Intense CCD cameras, a Solo 120 Nd:YAG double-pulsed laser, and a PC with dual Intel XEON processors running the Davis 7.1 PIV data acquisition and processing software. The Solo 120 laser was set up with a cylindrical lens with a focal length of $f = -10$ mm, which allowed a working distance of 2000 mm. This fulfills the distance requirement needed for the laser to properly illuminate the measurement area. A support mount for the laser was constructed which allowed the laser to be adjusted according to the location of the cameras. The support mount consists of a simple fixed rotation point located at the rear of the laser and two guide plates (one on each side of the laser; see Fig. 3). This allowed the laser to rotate to a +25° and a –5° from horizontal, while preventing any deviation of the laser sheet from the vertical plane of interest. Thus, the laser sheet would not deviate from the calibration plane.

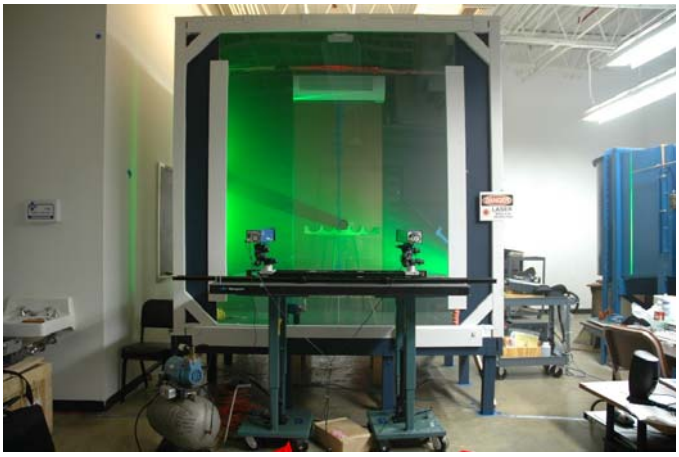

Fig. 2. Front view of the test cabin.

Fig. 3. Laser mount.

A safety concern was the movement of the laser while being aligned and fired. Even while wearing safety glasses, the laser beam can still have the potential of doing significant harm if it were to reflect into the eye, thereby damaging the retina. This typically was most problematic during calibration when the calibration plate was being aligned. Therefore, a Craftsman 180° laser level, with its lower laser power, was to simulate the laser sheet. The laser level was aligned with the PIV laser sheet such that the beam of the laser level is on the same path as that of the PIV laser. This alignment was performed by overlapping both laser beams at two different locations. This method provided a safer means of aligning the laser with the PIV laser turned off.

Fig. 4. The Lift Genie for vertically traversing the pair of cameras.

The two Flow Master 3S Image Intense CCD cameras were required to be arranged in such a way as to allow traversing along the *x* (left to right) and *y* (upward) axes. Budget limitations and the extensive traversing distance requirements for the large field-of-view prevented the use of an automated system. Thus, an alternate means of accomplishing this traversing requirement was needed. The solution resulted in the use of the Super Lift Advantage 15 (SLA-15) Lift Genie. This lift, shown in Fig. 4, is normally used in warehouse facilities to store large, heavy products at heights reaching 15 ft. The SLA-15 is capable of loads up to 800 lbs. The design configuration of the SLA-15 incorporated a vertical tilt angle of –2° which was undesirable, since the cameras required a 0° vertical ascent for maintaining their focal planes along the same plane as the laser sheet. However, the tilt was caused by the front casters; therefore, the tilt was removed by removing the front casters. The lift was operated by a manual two-speed winch with a rate of 11.5 cranks/ft for the low-speed setting.

The cameras were mounted on a 100 cm optical rail which, in turn, was mounted on a separate 300 cm optical rail; see Fig. 5. This setup allowed the cameras to traverse along the *x*-axis while maintaining the required separation distance as given by the requirements of stereo PIV.

III. Calibration

The calibration process used here is a method provided by the DaVis software known as the pinhole-fit model. This model is a mathematical model designed to project a 3-D image onto a 2-D plane. This process is somewhat similar to what is known in the art community as "linear perspective." During the calibration process, the position and orientation of each camera, relative to a calibration plate placed in the flow region, are estimated. With this method the projection from an actual three-dimensional object to the cameras' CCD chip is modeled. The basic concept of the pinhole fit is shown in Fig. 6.[17]

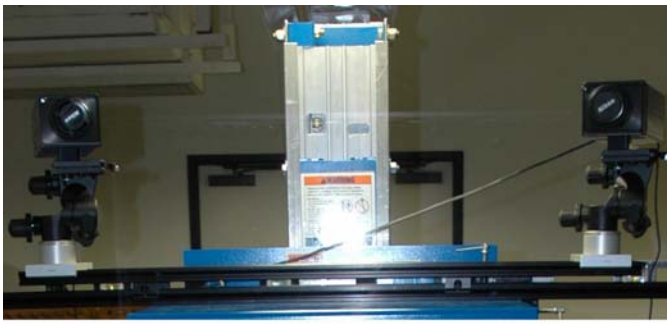

Fig. 5. Flow Master 3S Image Intense cameras in stereo arrangement.

The calibration results for the pinhole fit give useful geometric transformation information (rotation, translation, and RMS fit values) about each individual camera. A typical display of this information from the DaVis 7.1 software is given in Fig 7. The most important aspect of the calibration data is the RMS fit value. This value determines the accuracy of each camera's alignment to the calibration plate. Typical values for the RMS fit range from 1 to 10 pixels. Values above 10 pixels are considered questionable, while any value below 1 pixel is considered to be very accurate. Some other factors contained in the calibration data include the distance from the cameras to the area of interest (T_x, T_y, T_z), the rotation of each camera (R_x, R_y, R_z) with respect to the illuminated region (AOI), the size of the image, and the scale factor of the camera.

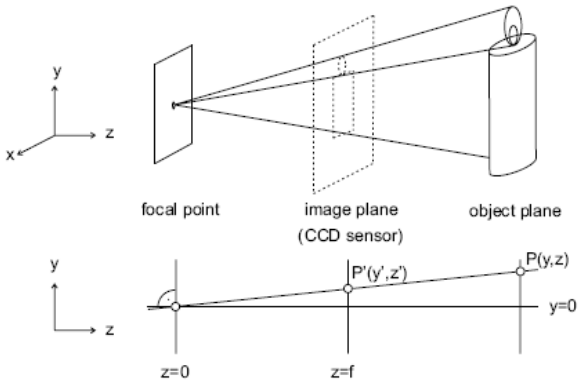

Fig. 6. Basic concept of the pinhole-fit model.[17]

IV. Data-Acquisition Process

PIV data acquisition and processing were controlled by the Davis 7.1 software. The first step was to determine the total area of interest (AOI) that could be captured by the stereo PIV setup. Due to the limited field of view of the stereo setup and the size of the AOI, the full 6 ft. by 8 ft. doorway region could not be imaged with the cameras in a single position. Instead, the AOI was split up into individual sections, that were imaged and then "stitched together."

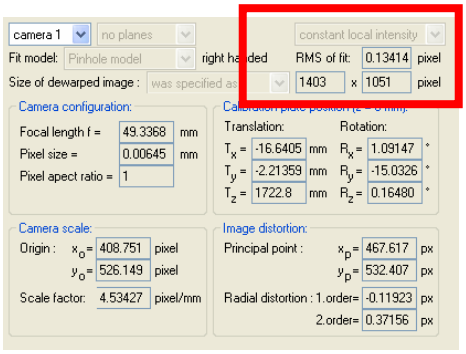

Fig. 7. Typical calibration results for the given setup.

The PIV camera field of view allowed a maximum of a 308 mm by 277 mm viewing area. Each viewing area was defined to be one rectangular grid. After the required number of images were obtained for a given rectangle (400 instantaneous images per location for the current work), the cameras were then translated horizontally to obtain data at the next rectangle. This process was repeated until PIV data for four rectangles were collected. These four rectangles, taken together, are equivalent to one row of data. Once a given row was completed, the cameras were then elevated to the next height using the Lift Genie in order to collect the required data for the next row. This process was repeated until all of the required data were obtained. The total number of rows examined was eight, such that a 32 grid rectangular area was measured (see Fig. 8). This appropriately covered the required AOI. Once the data were collected, the appropriate vector fields and average velocity profiles could be calculated for each individual rectangle. The data for these squares were then merged together according to the rectangle's specific locations, using capabilities provided by the DaVis 7.1 software.

V. Results

During the data collection process, several complications arose that needed close attention. The first complication arose in obtaining sufficient seeding. The seeding particles used were olive oil droplets which have a diameter of approximately 1.0 μm. For seeding the large volume of this air cabin, approximately 15 seconds of running the seeder with the air curtain on and one minute of air curtain runtime with the seeder off were needed so that the seeding particles would be evenly distributed throughout the cabin. It was noticed that over some time, the seeding density decreased. This reduction in seeding was thought to come from the absorption of the oil droplets into the wood frame of the cabin. This was first anticipated during the design phase of the cabin and a solution of applying paint was expected to help seal the wood to prevent this loss of seeding. The paint applied to the wood was two coats of a latex base sealant and two coats of flat black latex, but it was discovered that the seeding still penetrated the latex paint and absorbed into the wood. After several test runs were conducted, it was found that the seeding procedure described earlier would sustain sufficient seeding for an experiment time of approximately 45 minutes. If the seeder were run longer than this, saturation of the cameras would occur. Therefore, it was important to maintain the seeding within the appropriate range.

A second complication arose in elevating the cameras to obtain successive rows of data. The Lift Genie is designed with several tracks made of a steel alloy. This allowed for compact storage capability while still accomplishing the 15 ft. vertical traversing requirement. As the cameras were elevated, the manual crank was rotated approximately 20 revolutions for each row of data. However, when the next track was engaged, the rate at which the cameras ascend per revolution increased and therefore the required revolutions per row dropped to 8. This change plus stretching of the drive wire caused some uncertainty in the vertical position of the cameras. Even though the vertical positioning uncertainty from row to row was not too severe, it does demonstrate the necessity for accurate positioning. Future plans may call for a computer-automated traverse system that is more accurate in vertical positioning. This problem, however, did not occur when merging horizontally adjacent squares into rows. This can be explained by the fact that the cameras could be traversed horizontally along the optical rail with greater accuracy than could be achieved with the vertical traversing of the Lift Genie.

Within the image field of view, a thin shadow developed within which PIV data were difficult to collect. This shadow is due to a scratch that developed horizontally on the Plexiglas between the interior of the cabin and the laser. Several scratch removers were tried to remove this scratch. For one product in particular, the scratch appeared to be removed; however, the removal simply filled in the scratch and after polishing did not leave a flat surface. Instead, it left a concave dip within the crack. This concave dip resulted in the laser sheet being refracted from its path and thus still showed as a shadow during data acquisition.

The time required to obtain the vector fields for each rectangle, process the instantaneous images, and compute the average vector fields was approximately 16 hours. Upon completion of the calculations, the data for each rectangle were merged together manually into its designated row using the Davis 7.1 software, and then the rows were merged together to form the entire field. Row 8 (top row) was considered to be a primary vector profile since it determined if the flow leaving the air curtain was uniformly distributed along its length.

Figure 9 shows the ensemble-average velocity vector field for Row 8 just below the air curtain outlet. The vectors are colored by velocity magnitude. The vectors are seen to be directed essentially straight downward, as expected, with a maximum magnitude of approximately 5.5 m/s. Entrainment of ambient air at either side of the air curtain is also apparent in the figure. The corresponding velocity profile, for one particular vertical location approximately 10 mm below the air curtain outlet, is given in Fig. 10. This figure shows that the flow leaving the air curtain is relatively uniformly distributed along its length, which was accomplished with some adjustment of flow-conditioning devices within the diffuser leading to the air curtain inlet.

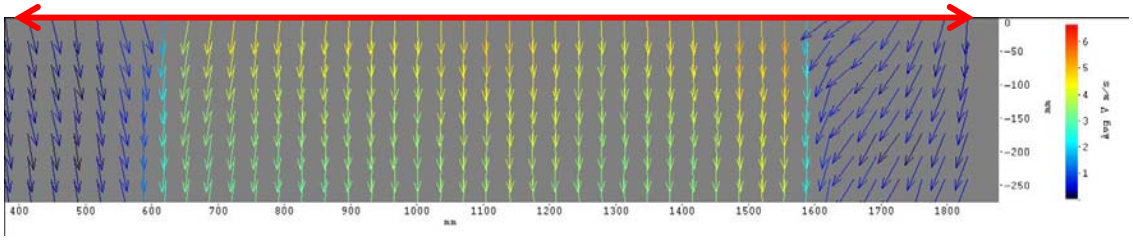

Fig 9. Velocity vector profile of row 8 after the data from the four side-by-side rectangles were merged together. The solid red line represents the location (10 mm from the bottom of the air curtain exhaust) where the data of Fig. 10 were obtained.

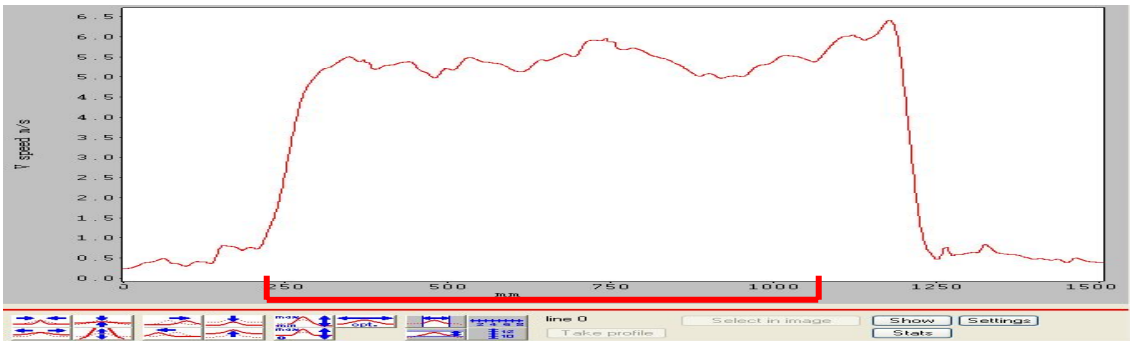

Fig 10. Plot of velocity profile for Row 8. The location of the profile is represented by the solid red line in Fig. 9.

Figure 11 shows the entire mean velocity vector field from the outlet of the air curtain down to the floor of the cabin. Again, the vectors are colored by velocity magnitude. The velocity vectors are predominantly oriented vertically downward with horizontal deflections near the floor that are inward toward the air exhaust vent and outward along the floor toward the outer edges of the image. Clearly, the exhaust vent is not long enough to capture the entire air curtain jet at the floor, as significant outward turning of the jet can be seen in the outside edge regions of the jet. Thus, the exhaust vent should be substantially larger for the EDP application than the one used here in order to capture the entire air curtain jet. The maximum jet velocity can also be seen to decrease as the jet traverses from the air curtain exhaust to the floor. This is due to entrainment of ambient air into the jet, or conversely, to diffusion of the jet into the ambient.

Figure 12 is a close up of the mean velocity vector field along the floor (Row 1) of the cabin. The turning of the jet flow into the air vent and outward along the floor can be seen clearly in this figure.

These last few figures demonstrate the ability of the current flow facility and PIV measurement system to characterize air curtain flows that are representative of the kinds of flows that could be used in EDPs. The air entering the exhaust vent could be sampled by sensors for the detection of explosives. To completely map this flow field, additional planes parallel to the current one (i.e., parallel to the plane of the air curtain jet) and also orthogonal to this plane should be examined both in the "clean" configuration examined here and with mannequins (or other objects) inserted into the jet to model humans walking though the air curtain. This is the subject of our ongoing work.

VI. Conclusions

With the ever-present threat of terrorism in our society, it is necessary to construct EDPs that are accurate, reliable, and non-intrusive. In order for the air to be collected and sampled properly, understanding the air flow within the portal becomes critical. Using PIV it is possible to map a large velocity vector field located near a doorway and below an air curtain, which is representative of an EDP flow. This method for mapping a doorway/air curtain flow does indeed have some areas of improvement that need to be addressed, but the current work shows the potential of obtaining large-field PIV measurements using a system that is generally applied to smaller-scale flows.

During the design phase of the air cabin, it was decided to use typical construction materials since they are inexpensive and readily available. During data collection, however, it was found that the wood would absorb the seeding particles and reduce the amount of seeding in the cabin over a relatively short period of time. After particularly long test runs of the cabin, the absorption of olive oil also tended to warp the wood to some extent. This warping was not particularly severe; however, it did require some minor maintenance. Further sealant applications or the use of a different sealant are needed to prevent long-term damage by the seeding absorption and loss of seeding during the experiments. Also, as in dealing with most lasers, no sealant that contains a gloss can be used because the laser sheet will reflect from it, causing potential harm to anyone in the testing area. It may not even be possible to prevent all of the seeding from being absorbed into the wood, but limiting the absorption would extend the time available for data collection.

Example PIV vector fields for the center plane of the air curtain jet in the test cabin have been presented. The large vector fields have been created by "stitching together" up to 32 smaller images in eight rows of four images each. These results show the applicability of the current methods for obtaining PIV measurements over the large fields typical of EDP flows.

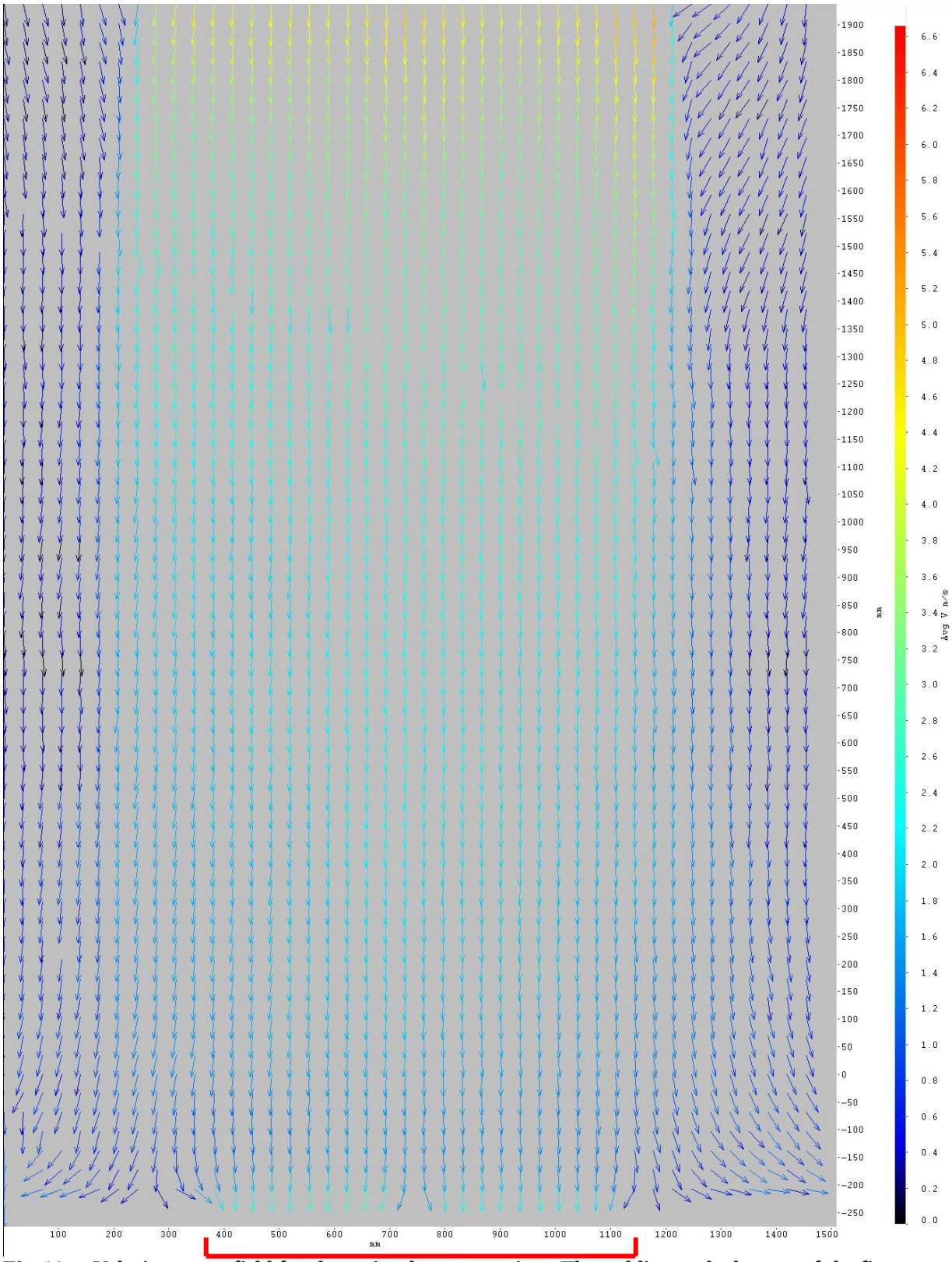

Fig. 11. Velocity vector field for the entire doorway region. The red line at the bottom of the figure represents the approximate location of the exhaust vent.

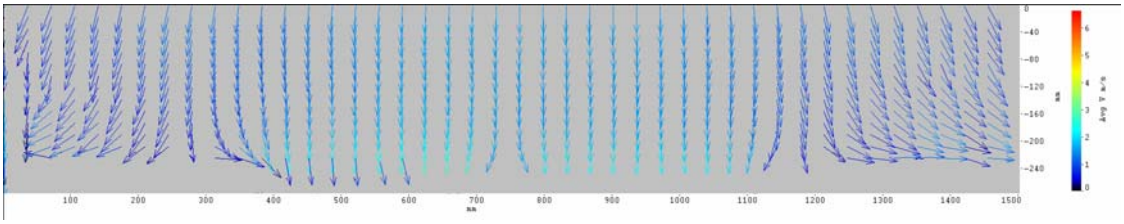

Fig 12. Velocity vectors for of Row 1 displaying the effect of the suction from the exhaust vent on the flow.

Further studies will involve mapping the doorway flow in multiple orthogonal planes to achieve a three-dimensional understanding of the flow. It is possible to use the same cameras and laser as used here, but in a different arrangement, to obtain results over these multiple planes. Future experiments will also include mannequins, and possibly other objects, to determine their effects on doorway-type flows and the potential influences on EDP design.

VII. Acknowledgements

The hardware for this project was made possible by the National Science Foundation's Major Research Instrumentation Grant No. 0421282 "Acquisition of Instrumentation for Engineering Research in Advanced Security Detection Systems."

VIII. References

[1]Hallowell, S. F., "Screening People for Illicit Substances: A Survey of Current Portal Technology," *Talanta*, Vol. 54, No. 3, 2001, pp. 447–458.

[2]Gowadia, H. A. and Settles, G. S., "The Natural Sampling of Airborne Trace Signals from Explosives Concealed upon the Human Body," *Journal of Forensic Sciences*, Vol. 46, No. 6, 2001, pp. 1324–1331.

[3]Settles, G. S., "Sniffers: Fluid-Dynamic Sampling for Olfactory Trace Detection in Nature and Homeland Security—The 2004 Freeman Scholar Lecture," *Journal of Fluids Engineering*, Vol. 127, No. 2, pp. 189–218, 2005.

[4]Parmeter, J. E., Linker, K. L., Rhykerd, C. L., Hannum, D. W. and Bouchier, F. A., "Explosives Detection Portal for High-Volume Personnel Screening," *Enforcement and Security Technologies*, edited by A. T. DePersia and J. J. Pennella, Proceedings of the SPIE, Vol. 3575, 1998, pp. 384–391.

[5]Rydock, J.P., Hestad, T., Haugen, H. Skaret, J.E., "An isothermal air curtain for isolation of smoking areas in restaurants," in Awbi, H.B., ed., *Air Distribution in Rooms, ROOMVENT 2000, Proceedings of the 7th International Conference on Ventilation for Health and Sustainable Environment*, 2000, Elsevier.

[6]Pavageau, M., Nieto, E.M. and Rey, C. "Odour and VOC Confining in Large Enclosures Using Air Curtains." *Water Science and Technology*, Vol. 44, No. 9, 2001, pp. 165–171.

[7]Edge, B. A., Paterson, E. G. and Settles, G. S., "Computational Study of the Wake and Contaminant Transport of a Walking Human," *Journal of Fluids Engineering*, Vol. 127, No. 5, 2005, pp. 967–977.

[8]Phillips, J. C. and Woods, A. N., "On Ventilation of a Heated Room Through a Single Doorway," *Building and Environment*, Vol. 39, No. 3, 2004, pp. 241–253.

[9]Lee, H. and Awbi, H. B., "Effect of Internal Partitioning on Indoor Air Quality of Rooms with Mixing Ventilation—Basic Study," *Building and Environment*, Vol. 39, No. 2, 2004, pp. 127–141.

[10]Moureh, J. and Flick, D., "Airflow Characteristics Within a Slot-Ventilated Enclosure," *International Journal of Heat and Fluid Flow*, Vol. 26, No. 1, 2005, pp. 12–24.

[11]Ampofo, F., "Turbulent Natural Convection in an Air Filled Partitioned Square Cavity, "*International Journal of Heat and Fluid Flow*, Vol. 25, No. 1, 2005, pp. 103–114.

[12]Foster, A. M., Swain, M. J., Barrett R. and James, S. J., "Experimental Verification of Analytical and CFD Predictions of Infiltration Through Cold Store Entrances," *International Journal of Refrigeration*, Vol. 26, No. 8, 2003, pp. 918–925.

[13]Sirén, K., "Technical Dimensioning of a Vertically Upwards Blowing Air Curtain—Part I," *Energy and Buildings*, Vol. 35, No. 7, 2003, pp. 681–695.

[14]Guyonnaud, L., Solliec, C., Dufresne de Virel, M. and Rey, C., "Design of Air Curtains Used for Area Confinement in Tunnels," *Experiments in Fluids*, Vol. 28, No. 4, 2000, pp. 377–384.

[15]Rouaud, O., Havet, M. and Solliec, C., "Influence of External Perturbations on a Minienvironment: Experimental Investigations," *Building and Environment*, Vol. 39, No. 7, 2004, pp. 863–872.

[16]Hu, S.C., Chuah, Y.K. and Yen, M.C., "Design and Evaluation of a Minienvironment for Semiconductor Manufacture Processes," *Building and Environment*, Vol. 37, No. 2, 2002, pp. 201–208.

[17]"LaVision PIV System User's Manual," LaVision Inc., 2005.